13th International Conference on Applications of Statistics and Probability in Civil Engineering, ICASP13
Seoul, South Korea, May 26-30, 2019

Risk-based Design of an Offshore Wind Turbine using VoI Analysis

Jorge Mendoza
PhD student, Department of Structural Engineering, Norwegian University of Science and Technology, Trondheim, Norway

Jochen Köhler
Professor, Department of Structural Engineering, Norwegian University of Science and Technology, Trondheim, Norway

ABSTRACT: Monopiles are the most common solution for supporting wind turbines in offshore conditions. At the design phase of a monopile, a frequency check is to be performed to avoid the resonance hazard with the 1P and 3P excitation, i.e. the frequency domains at which the rotor provokes excitations. However, the estimation of the first natural frequency of the structure is associated with large uncertainties, especially due to lack of knowledge about the soil-structure interaction. Resonance with the dynamic excitations results in a reduced fatigue life. In this paper, the frequency check is addressed following a probabilistic formulation. A rational decision framework is proposed to find an optimum design, based on the evaluation of the expected consequences of failure using risk metrics. Furthermore, the value of acquiring further site-specific information on the soil characteristics is addressed by means of a value of information analysis. A Bayesian network is developed to represent the system and facilitate the analysis. The results provide insight on (1) the relation between design parameters and the risk associated with dynamic amplifications; and (2) how to efficiently distribute the resources at the design point in time.

1. INTRODUCTION

Monopiles are the preferred offshore wind turbine (OWT) support structure (Remy and Mbistrova, 2018). Optimization of the support structure design is essential for the purpose of reducing the levelized cost of wind energy and thus, keeping the growing trend of the technology (McAuliffe et al., 2017).

OWTs are complex structural systems subject to several sources of dynamic loading, which may induce dynamic amplification of the structural response. According to guidelines, such as DNV-GL (2016b), the structural design of an OWT is to verify that resonance with the rotor (1P) and blade-passing (3P) excitations is avoided. This is addressed with a frequency check, in which a deterministic minimum acceptable margin between the estimated natural frequencies of the OWT and the excitation regions is imposed. However, evidence exists of this type of resonance happening in operational conditions (Hu et al., 2014). Mitigating this issue in operational conditions instead of during the design phase is associated with higher costs and risk. Therefore, the deterministic frequency check is not sufficient. A more thorough study of the limitations of this approach can be found in Mendoza and Köhler (2019). This motivates the development of alternative methodologies, in which the risk associated with a certain design is assessed explicitly.

For a three-bladed pitch-controlled wind turbine, the frequency domain can be divided into five regions, which are synthesized in the form of a Campbell diagram in Figure 1. Note that Ω_0 and Ω_r are the cut-in and rated rotor speeds, respectively. The regions are, from smaller to larger frequencies, (1) the soft-soft region; (2) the 1P region; (3) the soft-stiff region; (4) the 3P region; and (5) the stiff-stiff region. Designs whose first natural frequency f_{n1} lies in the soft-soft region do not provide enough

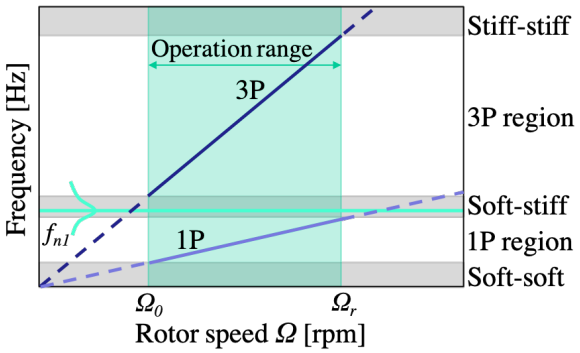

Figure 1: Campbell diagram illustrating the rotor and blade-passing excitation regions.

stiffness, meaning that the flexibility of the compliant structure is detrimental for stable energy production and for the fatigue life of the mechanical components in the rotor-nacelle assembly. Designs in the stiff-stiff region are not cost-efficient. Therefore, the design space is restricted to the soft-stiff region in general. The prediction of the natural frequencies of the OWT at the design phase is associated with large uncertainties. The uncertainty can be understood as composed from an epistemic and a stochastic part. The epistemic part is associated, among others, to the uncertainty in the estimation of soil parameters, the depths of soil stratification, and the soil-structure interaction modeling. The stochastic uncertainty becomes larger the further in time from the estimation point in time and cannot be fully reduced by acquiring further information. Examples are the scour development, or the soil softening or stiffening (Schafhirt et al., 2016).

At the design stage, there are several ways of dealing with the uncertainties mentioned above. On the one hand, the design can be over-engineered in order to compensate the state of imperfect information. This strategy is commonly used in practice. However, as the extension of the soft-stiff region becomes narrower for larger wind turbine rotors, an over-engineered design may yield a first natural frequency close to or in the 3P region. On the other hand, it is possible to partially reduce the uncertainties by acquiring information. In general, a compromise between the two mentioned possibilities should be pursued in order to manage the risk at minimum cost and maximum revenue.

In this paper, a risk-based decision framework is developed with the following two objectives: (1) to determine a cost-effective design based on available prior information and (2) to quantify the value of additional information procured by testing the site-specific soil condition. In the following section, the methodology used to address the objectives is described. The characteristics of the numerical model employed to implement the methodology is documented in Section 3. The results are presented in Section 4. The main conclusions and the future outlook are reported in Section 5.

2. METHODS

A risk-based decision framework is proposed to asses the expected consequences of the resonance hazard with the 1P and 3P regions. The optimum design is evaluated using utility theory (von Neumann and Morgenstern, 1966). The decision variables are the design parameters. Two design parameters are considered: the monopile diameter and thickness at a reference height. A parametric definition of the structure is developed based on the two design parameters, so that a combination of the two defines a monopile design. This is further explained in the following section. A discrete set of designs $\mathbf{d_s} = \{d_1, d_2, ..., d_n\}$ is generated, constituting the design decision vector. The optimum design d_{opt} is found according to Eq. (1), i.e. by minimizing the expected total cost $E[C_T|\mathbf{d_s}]$.

$$d_{opt} = \underset{d_{opt} \in \mathbf{d_s}}{\arg\min} \{E[C_T|\mathbf{d_s}]\} \tag{1}$$

The expected total cost is computed using Eq. (2). The costs of manufacturing a cylindrical and a conical section are set to 2€/kg and 3€/kg, respectively, according to the cost model in De Vries et al. (2011). The failure costs are set to $C_f = 2C_c$ in this example.

$$E[C_T] = C_c + E[C_f] = C_c + C_f P_f \tag{2}$$

In general, structural resonance with the wave loading and the 1P and 3P excitations do not cause structural failure due to the high aerodynamic damping. Nevertheless, it results in dynamic amplifications and therefore, an increase of the fatigue failure risk. Due to this, the failure risk $E[C_f]$

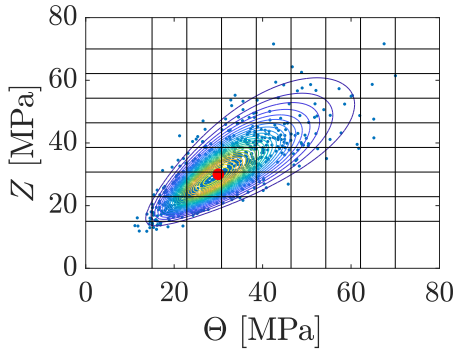

Figure 2: Likelihood function $L(\theta)$ between the outcome of the soil test Z and the true state of the soil modulus of elasticity Θ.

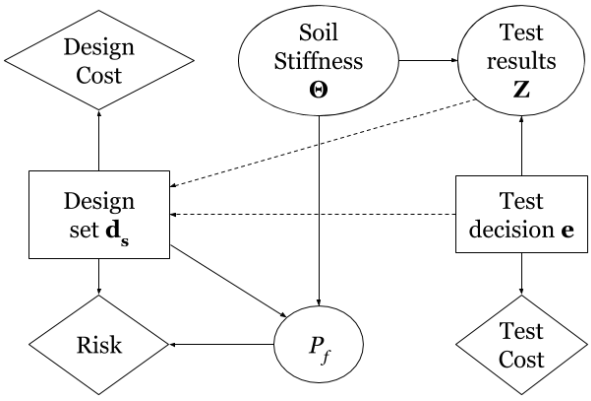

Figure 3: Influence Diagram used for the VoI analysis.

is studied through a fatigue limit state by using Eq. (3) (JCSS, 2001). Note that g_{fat} is the limit state function, P_f is the probability of failure and Δ is the uncertain Miner's sum at failure, defined by a Log-Normal with parameters $\mu_\Delta = 1$ and $\sigma_\Delta = 0.3$. The soil is represented, given prior knowledge, by a single sand stratum with modulus of elasticity E_{soil} following a Log-Normal with expected value equal to 30 MPa and coefficient of variation of 0.3. A multiplicative model uncertainty X, associated to the uncertainty in the soil-structure interaction model used to estimate the first natural frequency f_{n1}, is applied. X is represented by a Log-Normal with parameters $\mu_X = 1$ and $\mu_X = 0.05$. The other basic variables are represented deterministically.

$$P_f = \Pr[g_{fat} \leq 0] = \Pr[\Delta - FLD(f_{n1}) \leq 0] \quad (3)$$

A value of information (VoI) analysis (Raiffa and Schlaifer, 1961) is performed in order to quantify the economic value of testing the soil site-specific characteristics. Two testing options are considered $\mathbf{e} = \{e_0, e_1\}$: (e_0) To not invest in acquiring new information, and (e_1) To test the soil site-specific conditions in order to reduce the epistemic uncertainties associated to E_{soil}. The net VoI V^* is computed using Eq. (4), where $E[C_T|e_1, \mathbf{d_s}]$ is the preposterior expected total cost.

$$V^* = E[C_T|e_0, d_{opt}] - E[C_T|e_1, \mathbf{d_s}] \quad (4)$$

In order to compute $E[C_T|e_1, \mathbf{d_s}]$, a likelihood $L(\theta)$ of the test outcomes Z is formulated, see Eq. (5). Note that θ refers to the true state of the soil modulus of elasticity. In this example, due to the absence of empirical data, $L(\theta)$ is defined by a multivariate Log-Normal with mean value vector $\mu_{\Theta,Z} = [30, 30]^{\mathrm{T}}$ [MPa], a correlation $\rho_{\Theta,Z} = 0.8$ and standard deviations $\sigma_\Theta = \sigma_Z = 9$ MPa.

$$L(\theta) = \Pr[Z|\Theta = \theta] \quad (5)$$

The influence diagram (ID) illustrated in Figure 3 is implemented in GeNIe© to evaluate V^*. All the nodes are discretized. $L(\theta)$ is discretized to 9 test outcome intervals.

3. DESCRIPTION OF THE NUMERICAL MODEL

A simplified numerical model is developed to estimate the fatigue damage given a realization of the first natural frequency of the structure. This is later used to estimate the probability of failure and ultimately, the risk. The risk is employed as a decision ranking metric, taking basis on utility theory. Therefore, it is not pursued to develop a complex, computationally expensive model that captures the detailed behaviour of the structure. On the contrary, a sufficiently complete model that enables the assessment of the structural behavior that affects the considered design decisions is preferred. The dynamic behaviour of the OWT is to be modelled in the time domain in order to evaluate the cumulative fatigue damage. In the following, the parametric definition of the design and the employed numerical model are documented.

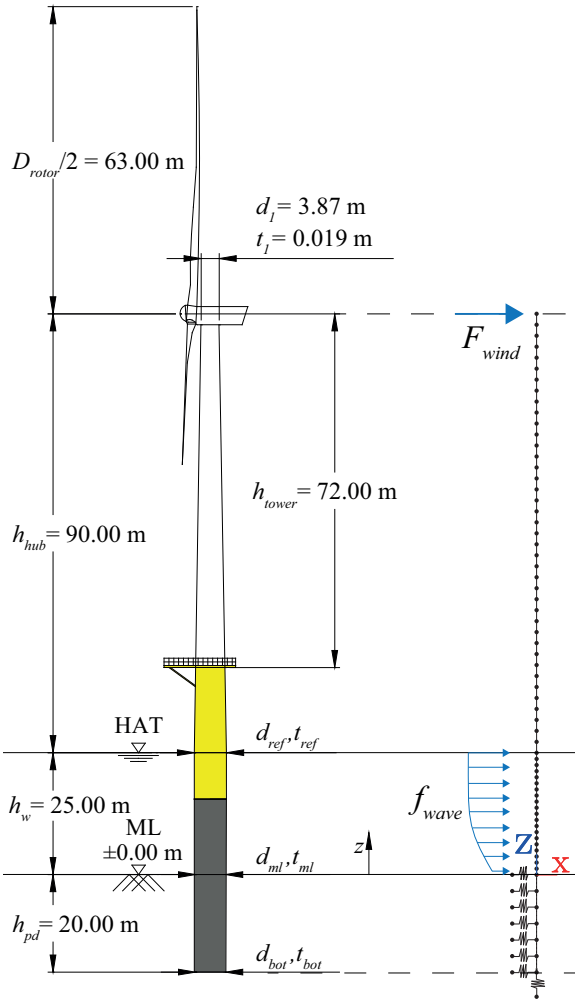

Figure 4: Illustration of the parametric description of the design and the numerical model.

3.1. Design set

A set $\mathbf{d_s}$ of 12 designs is built based on a parametric definition of an OWT. A design is given by the specification of two design parameters, the diameter d_{ref} and the thickness t_{ref} at a reference location. The Matlab© FE toolbox StaBIL2.0 is used to develop a numerical model of the OWT structure. The 5-MW NREL reference wind turbine is employed (Jonkman et al., 2009). For this turbine, the cut-in and rated rotor speeds are $\Omega_0 = 0.1150$ Hz and $\Omega_r = 0.2017$ Hz, respectively. A sketch of the OWT parametric definition and the numerical model is presented in Figure 4. The following should be noticed. A linear transition of both the diameter and thickness is set between the two mentioned cross-sections. The connection between the tower and the monopile is assumed to be perfect. Secondary steel components, such as boat landing, are not explicitly included in the analysis. The added mass of the secondary steel is taken into account by setting the steel density to 8500 kg/m^3. The cross-section of the monopile is kept constant from h_w up to the penetration depth, i.e. h_{pd}. The design set is defined in Table 1.

Table 1: Definition of the reference diameter d_{ref} and thickness t_{ref} for the design set $\mathbf{d_s}$ used in this study.

Design #	d_{ref}	t_{ref}
d_{s1}	5.50 m	0.055 m
d_{s2}	5.80 m	0.058 m
d_{s3}	6.25 m	0.063 m
d_{s4}	6.60 m	0.067 m
d_{s5}	7.00 m	0.070 m
d_{s6}	7.20 m	0.072 m
d_{s7}	5.50 m	0.058 m
d_{s8}	5.80 m	0.061 m
d_{s9}	6.25 m	0.066 m
d_{s10}	6.60 m	0.069 m
d_{s11}	7.00 m	0.073 m
d_{s12}	7.20 m	0.075 m

The soil-structure interaction is modelled by a set of linear springs with stiffness equal to the modulus of subgrade reaction k_s. The formulation of this simple model was firstly proposed in Winkler (1867). There is no agreement in the literature regarding the relation between k_s and the soil modulus of elasticity E_{soil}. This issue is investigated by comparing the 1-D model with more sophisticated 3-D FE models in Rani and Prashant (2014). It is concluded that the relation $k_s = 2E_{soil}$, proposed in Muscheliśvili (1953), gives reasonable results. Due to that and its simplicity, this relation is used in this study. The relation between realizations of E_{soil} and the first natural frequency of the structure f_{n1} is mapped using the numerical model, see Figure 5.

3.2. Environmental loading

The dynamic analysis performed in this study is carried out in the time domain. The environmental loading is computed for eleven fatigue load cases (FLCs) from 1-hour time series of the sea state.

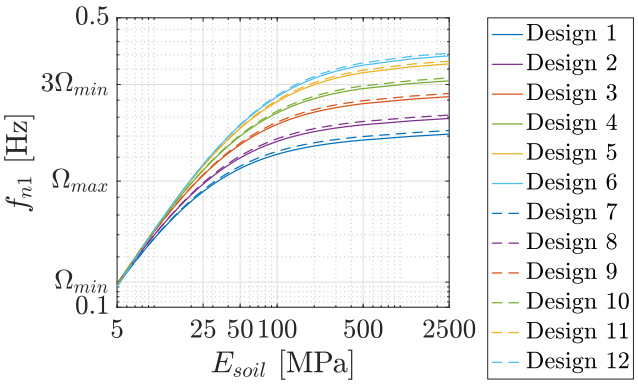

Figure 5: Relation between the soil modulus of elasticity E_{soil} and the first natural frequency f_{n1} for the considered designs.

The FLCs are taken from the K13 shallow water site (Fischer et al., 2010), where the stochastic wind was fitted to a Weibull distribution with parameters $A = 11.31$ m/s and $k = 1.97$. The lumped sea states are defined by four parameters: the 10-min average wind speed at hub height V_{10}, the turbulence intensity I, the significant wave height H_s and the peak period T_p. The wind bins are set to 2 m/s. The probability of occurrence of the wind bins $f_V(v)$ is scaled to fit the cut-in and cut-out wind speeds of the 5-MW NREL wind turbine. Since the purpose of the dynamic analysis is to estimate the fatigue damage, the load effects induced by non-cyclic sources, such as currents, are neglected.

The wind time series are generated by inverse Fourier transform of the wind spectrum, which is chosen to be the Karman spectrum (von Karman, 1948). The Karman spectrum is modified to account for rotational sampling. This is done in order to model the 1P and 3P excitations in a simplified manner, so that computationally expensive aero-elastic simulations are avoided. The modified Karman spectrum $S_w(f)$ is the Fourier transform of the autocorrelation function $R_{11}(\tau)$ derived in Connell (1982), cf. Eqs. (6) and (7). Note that D_{Rotor} is the rotor diameter, L_u is the turbulence length, which is set to 340.2 m, Γ is the gamma function and K_ν is the modified Bessel function of the second kind of order ν.

$$S_w(f) = 4\int_0^\infty R_{11}(\tau)\cos(2\pi f\tau)\mathrm{d}\tau \qquad (6)$$

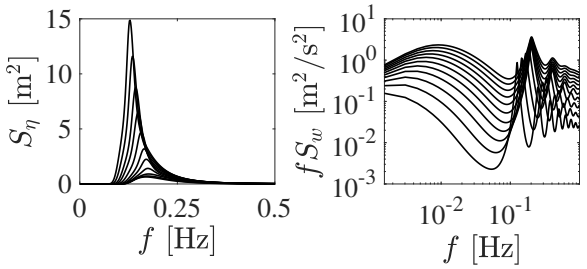

Figure 6: Spectra used to generate the environmental loading: JONSWAP spectra S_η and Karman spectra S_w accounting for rotational sampling.

$$R_{11}(\tau) = \frac{2(V_{10}I)^2}{\Gamma(1/3)}(\kappa/2)^{1/3}\cdot\Big[K_{1/3}(\kappa) - \kappa/2\cdot K_{2/3}(\kappa)\left(\frac{4D_{Rotor}\sin(\Omega\tau/2)}{5s}\right)^2\Big] \qquad (7)$$

With κ and s defined as:

$$\kappa = \frac{s}{1.34L_u}$$
$$s = \sqrt{V_{10}^2\tau^2 + \frac{16}{25}D_{Rotor}^2\sin^2(\Omega\tau/2)} \qquad (8)$$

The JONSWAP spectrum is used to generate the wave time series. The different wind and wave spectrums used to generate the 11 lumped sea states are illustrated in Figure 6.

3.3. Dynamic response

The dynamic model takes basis on the simplified numerical model in Schløer et al. (2018). Only the in-plane deflections are considered. The dynamic response of the system is assumed to be represented accurately enough by the first mode of vibration. Hence, the dynamic horizontal displacement u is approximated by $u \approx \alpha_1\phi_1$, with ϕ_1 and α_1 being the first mode shape and the generalized coordinate of the first mode of vibration, respectively. The equation of motion of the system can then be described by Eq. (9). The generalized mass GM_1, stiffness GK_1, damping GD_1 and force GF_1 are defined in Eqs. (10) to (13); where ζ is the damping ratio and $\mathbf{M}$ and $\mathbf{K}$ are the mass and stiffness matrices, respectively.

$$GM_1\ddot{\alpha}_1 + GD_1\dot{\alpha}_1 + GK_1\alpha_1 = GF_1 \tag{9}$$

$$GM_1 = \phi_1^{\mathrm{T}}\mathbf{M}\phi_1 \tag{10}$$

$$GK_1 = \phi_1^{\mathrm{T}}\mathbf{K}\phi_1 \tag{11}$$

$$GD_1 = \frac{\zeta GK_1}{\pi f_{n1}} + 2\zeta\sqrt{GM_1 \cdot GK_1} \tag{12}$$

$$GF_1 = \phi_1(z_{hub})F_{wind} + \int_{z_{ml}}^{z_{hub}} f_{wave}\phi_1 \mathrm{d}z \tag{13}$$

The stress at mudline S is used as a proxy of the maximum stress of the monopile, which in general occurs at a cross-section embedded in the soil. S is computed from the bending moment at mudline $M_y(z_{ml})$ defined in Eq. (14), assuming linear-elastic behaviour of the steel. The shear induced stress is neglected.

$$\begin{aligned} M_y(z_{ml}) &= F_{wind}\cdot(h_{hub}+h_w)+ \\ &\int_{z_{ml}}^{z_0} f_{wave}(z)z\mathrm{d}z - \int_{z_{ml}}^{z_{hub}} \rho\ddot{\alpha}_1\phi_1 z\mathrm{d}z \end{aligned} \tag{14}$$

3.4. Fatigue resistance

The fatigue resistance is computed following the SN-curve methodology as described in DNV-GL (2016a). The relation between a certain stress range and the number of cycles to failure is given by Eq. (15). The parameters $\log\bar{a}_i$, m_i and k are set as for the D-curve. The sub-index i refers to the first ($i=1$) or second part ($i=2$) of the two slopped piece-wised SN-curve definition. Eq. (15) can be reorganized as in Eq. (16) to account for stress amplitudes $\sigma/2$. This is required since the rainflow counting algorithm is used to identify and group stress amplitudes into cycles and semi-cycles.

$$\log N = \log\bar{a}_i - m_i\log\left(S\left(\frac{t}{t_{ref}}\right)^k\right) \tag{15}$$

$$N\left(\frac{\sigma}{2}\right)^{m_i} = 10^{\log\bar{a}_i}\cdot 2^{-m_i}\cdot\left(\frac{t}{t_{ref}}\right)^{-k\cdot m_i} \tag{16}$$

The fatigue damage caused by each loading cycle or semi-cycle is defined as the ratio in Eq. (17). The Palmgren-Miner superposition is adopted (Miner, 1945). The life-time fatigue damage FLD is computed using Eq. (18), in which the fatigue damage estimated from the 1-hour simulations T_{sim} is weighed with the probability of occurrence of each of the eleven FLCs $f_V(v_{j_2})$ and scaled to the 20-year service life T_{life}.

$$D_{j_1} = \frac{n_{j_1}S_{j_1}^{m_i}}{N\left(\frac{\sigma}{2}\right)^{m_i}} = \frac{1}{10^{\log\bar{a}_i}}\cdot 2^{m_i}\cdot\left(\frac{t}{t_{ref}}\right)^{k\cdot m_i} \tag{17}$$

$$FLD = \frac{T_{life}}{T_{sim}}\sum_{j_2=1}^{11}\left(\sum_{j_1\in 1\mathrm{h}} D_{j_1,j_2}\right) f_V(v_{j_2}) \tag{18}$$

4. RESULTS AND DISCUSSION

The probability density functions of the first natural frequency $f_{F_{n1}}(f_{n1})$ are plotted in Figure 7. Note that the relation between f_{n1} and E_{soil} presented in Figure 5 and the model uncertainty X are used for their computation.

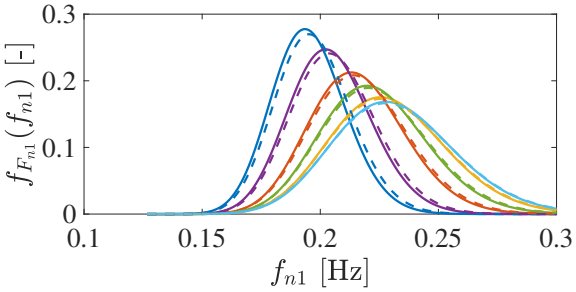

Figure 7: Probability density function of the first natural frequency $f_{F_{n1}}(f_{n1})$ based on prior soil parameters. The colour scheme corresponds to Figure 5.

The results of the estimation of the fatigue life damage FLD are presented in Figure 8. An increase of the FLD can be observed within the 1P region, having its maximum value when $f_{n1}\approx\Omega_r$. This reflects the importance of the effect of the resonance on the fatigue life. Considering e.g. d_{s1}, a realization of $f_{n1}\approx 0.2$ Hz results in double the FLD as a realization of $f_{n1}\approx 0.26$ Hz; or in other words the design is expected to fail at half the time, since FLD is inversely proportional to the fatigue life. Furthermore, it is observed that the resonance effect influences a large frequency range within the soft-stiff region.

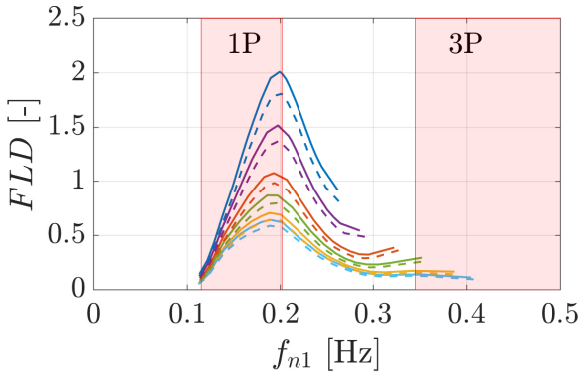

Figure 8: Fatigue life damage (FLD) for each realization of f_{n1} of the tested design set. The colour scheme corresponds to Figure 5.

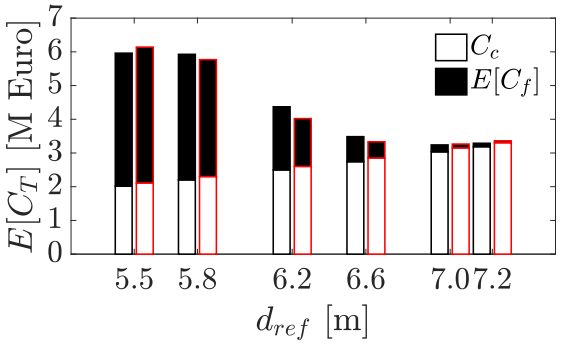

Figure 10: Expected prior total cost $E[C_T]$. Black-edged bars correspond to designs with reference thickness $t_{ref} = d_{ref}/100$, i.e. d_{s1} to d_{s6}; and red-edged bars to $t_{ref} = d_{ref}/100 + 0.003$ m, i.e. d_{s7} to d_{s12}.

The expected fatigue life damage $E[FLD]$ and the probability of failure P_f given prior knowledge are plotted in Figure 9 as a function of d_{ref}. The expected total cost $E[C_T]$ is plotted in Figure 10. It can be seen that $P_f \approx 1$ for the designs d_{s1} and d_{s7}. This was expected since the expected value of f_{n1} for these designs is ca. 0.197 Hz, i.e. it lies in the 1P region. Furthermore, it can be observed that the additional investment needed to realize the design d_{s2} in comparison to d_{s1} does not compensate the risk reduction, since the expected cost remains almost constant. The optimum design given prior knowledge is found to be the design d_{s5}, which is defined by $d_{ref} = 7.00$ m and $t_{ref} = 0.07$ m. The minimum prior expected cost is then computed to be $E[C_T|e_0, d_{s5}] = 3.239$M€.

The preposterior expected total cost $E[C_T|e_1, \mathbf{d_s}]$ is computed using the likelihood function of the soil testing technology, see Figure 2. The minimum value of $E[C_T|e_1, \mathbf{d_s}]$ results in 3.198M€. The net VoI follows then from Eq. (4), resulting in $V^* = 41000$ €. This value is significantly smaller than what it would be required for testing the soil in offshore conditions. Nevertheless, the system effects associated to considering the complete wind farm and the added value provided by informing decisions that regard other failure modes are not included in this study. This is further discussed in the following section.

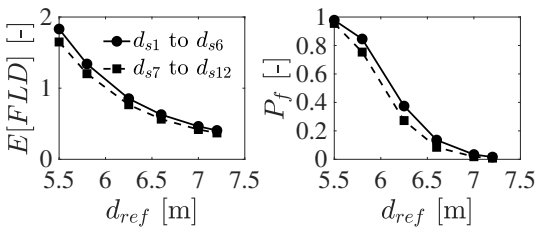

Figure 9: Expected fatigue life damage $E[FLD]$ and Probability of failure P_f given prior soil parameters.

5. CONCLUSIONS

A risk-based framework to inform decisions for the design phase of OWTs was presented in this paper. In particular, the study focuses on quantifying the risk due to the resonance hazard with the rotor and blade-passing excitations. The risk was quantified by defining a fatigue limit state. A simplified case study was regarded to showcase the methodology.

First, the optimum design was assessed utilizing available prior information. Insight regarding the optimum dimensions of the monopile support structure was provided. These results were then used to estimate the value of information of testing the site-specific soil conditions. The obtained net value of information is significantly smaller than the cost of a typical offshore soil testing campaign. Nevertheless, this study considered a single OWT rather than an offshore wind farm. Taking into account the wind farm system effects may have a significant impact in the results. Information could be used to update the spacial variability of the soil properties and the estimated prior correlation between the soil characteristics at different locations within the wind farm. Additionally, the comparison of the

computed value of information and the costs of performing a soil campaign could be compared in a fair manner. It should be noted that the benefit of inspecting the soil conditions are broader than just updating the knowledge regarding the soil parameters. For instance, the value of hazard identification on the seabed should be included in the analysis.

Further research regarding the application of the value of information analysis to design decisions should follow this study. Future investigations may include the collection of empirical soil data to build the likelihood function and the modelling of the system effects to compute the value of information. The studies should address the sensitivity of the analysis regarding the cost model and the modelling of the uncertainty.

6. REFERENCES

Connell, J. R. (1982). "Spectrum of wind speed fluctuations encountered by a rotating blade of a wind energy conversion system: observations and theory." *Solar Energy*, 29(5), 363–375.

De Vries, W. E., Vemula, N. K., Passon, P., Fischer, T., Kaufer, D., Matha, D., et al. (2011). "Final report WP 4.2: support structure concepts for deep water sites: deliverable D4. 2.8." *Report no.*, WP4: offshore foundations and support structures.

DNV-GL (2016a). "Fatigue design of offshore steel structures." *Standard DNVGL-RP-C203*, DNV-GL.

DNV-GL (2016b). "Support structures for wind turbines." *Standard DNVGL-ST-0126*, DNV-GL.

Fischer, T., De Vries, W. E., and Schmidt, B. (2010). "UpWind design basis (WP4: Offshore foundations and support structures)." *resreport*, UpWind project.

Hu, W.-H., Thöns, S., Said, S., and Rücker, W. (2014). "Resonance phenomenon in a wind turbine system under operational conditions." *structural health monitoring*, 12, 14.

JCSS (2001). "Probabilistic model code. part 3: Resistance models." *Standard*, Joint Committee of Structural Safety.

Jonkman, J., Butterfield, S., Musial, W., and Scott, G. (2009). "Definition of a 5-MW reference wind turbine for offshore system development." *National Renewable Energy Laboratory, Golden, CO, Technical Report No. NREL/TP-500-38060*.

McAuliffe, F. D., Murphy, J., Lynch, K., Desmond, C., Norbeck, J. A., Nonås, L. M., Attari, Y., Doherty, P., Sorensen, J. D., et al. (2017). "Driving cost reductions in offshore wind." *Report no.*, Leanwind.

Mendoza, J. and Köhler, J. (2019). "Value of site-specific information for the design of offshore windfarms." *IABSE Symposium 2019 Guimarães*.

Miner, M. A. (1945). "Cumulative damage in fatigue." *Journal of Applied Mechanics*, 12(3), 159–164.

Muschelišvili, N. I. (1953). *Some basic problems of the mathematical theory of elasticity: fundamental equations, plane theory of elasticity, torsion and bending*. Springer.

Raiffa, H. and Schlaifer, R. (1961). *Applied statistical decision theory*. Cambridge University Press.

Rani, S. and Prashant, A. (2014). "Estimation of the linear spring constant for a laterally loaded monopile embedded in nonlinear soil." *International Journal of Geomechanics*, 15(6), 04014090.

Remy, T. and Mbistrova, A. (2018). "Offshore wind in Europe. Key trends and statistics 2017." *techreport*, Wind Europe.

Schafhirt, S., Page, A., Eiksund, G. R., and Muskulus, M. (2016). "Influence of soil parameters on the fatigue lifetime of offshore wind turbines with monopile support structure." *Energy Procedia*, 94, 347–356.

Schløer, S., Castillo, L. G., Fejerskov, M., Stroescu, E., and Bredmose, H. (2018). "A model for quick load analysis for monopile-type offshore wind turbine substructures." *Wind Energy Science*, 3, 57–73.

von Karman, T. (1948). "Progress in the statistical theory of turbulence." *Proceedings of the National Academy of Sciences of the United States of America*, 34(11), 530.

von Neumann, J. and Morgenstern, O. (1966). *Theory of games and economic behavior*. Princeton university press, third edition.

Winkler, E. (1867). *Die Lehre von der Elasticitaet und Festigkeit*, Vol. 1. Dominicus.